Smart Structures and Systems, *Vol. 28, No. 4 (2021) 483-497*
https://doi.org/10.12989/sss.2021.28.4.483

xShake: Intelligent wireless system for cost-effective real-time seismic monitoring of civil infrastructure

Yuguang Fu*[1], Tu Hoang [2a], Kirill Mechitov [3b], Jong R. Kim [4c], Dichuan Zhang [4d] and Billie F. Spencer, Jr. [2c]

[1] *School of Mechanical Engineering, 585 Purdue Mall, West Lafayette, IN 47907, USA*
[2] *Department of Civil and Environmental Engineering, University of Illinois at Urbana-Champaign, 205 N. Matthews Ave., Urbana, IL 61801, USA*
[3] *Department of Computer Science, University of Illinois at Urbana-Champaign, 201 North Goodwin Avenue, Urbana, IL 61801, USA*
[4] *Department of Civil and Environmental Engineering, Nazarbayev University, Astana 010000, Kazakhstan*

(*Received August 13, 2020, Revised May 15, 2021, Accepted July 28, 2021*)

Abstract. Seismic structural health monitoring (SHM) of structures is critical not only to detect earthquakes to send early warning, but also to enable rapid structural condition assessment to ensure safety. Traditional monitoring systems using wired sensors are expensive. Wireless sensors offer tremendous opportunity to reduce costs, which remains elusive for seismic structural monitoring due to two main obstacles. First, there are constraints on power resources. Most wireless sensors are duty-cycled to preserve limited battery power; and hence, can miss an earthquake in power-saving sleep mode. Second, there is a lack of support for rapid post-event data collection and processing. Conventional data transmission after sensing can introduce significant delays, and real-time data acquisition that eliminates these delays has limited throughput. In this paper, an intelligent wireless monitoring system, *xShake*, is developed for cost-effective real-time seismic SHM. It consists of: 1) energy-efficient wireless sensor prototypes utilizing on-demand sensing technique, 2) live-streaming framework that supports high-throughput real-time data acquisition, and 3) a rapid condition assessment application, enabling real-time data visualization and processing for end users. The performance of the *xShake* is validated through lab tests, demonstrating that it can capture high-fidelity synchronized data under earthquakes and enable real-time structural condition assessment.

Keywords: earthquake monitoring; rapid condition assessment; real-time systems; structural health monitoring; wireless smart sensors

1. Introduction

Earthquakes are very difficult to predict, and their major shock is usually very short. However, they can result in significant structural damage and casualties. For example, in the Central Mexico earthquake, while the major shock only lasted about 20 seconds, it seriously damaged more than 3,000 buildings, resulting in 6,011 injuries and 370 deaths (McDonnell *et al*. 2017). Therefore, the development of monitoring systems is of great importance to not only enable earthquake detection, but also to facilitate rapid condition assessment of civil infrastructure. They are very useful for seismic events with many aftershocks in a brief period, as they can help to address the public concerns about structural safety during each aftershock, providing enough information to make informed decisions (Çelebi 2013).

Conventionally, wired sensors are employed for seismic monitoring of civil infrastructure, such as gas pipelines, traffic systems, bridges and buildings (Yamazaki *et al*. 1994, Yamazaki 2001, Celebi 2006, Okada *et al*. 2009). However, these monitoring systems have an averaged installed system cost of ranging from $5K to $20K per channel (Celebi 2006, 2013), which is prohibitive to widely instrument most of the structures in earthquake-prone areas. In contrast to wired counterparts, wireless smart sensors (WSS) are an attractive alternative, because they have much lower costs and hence realize the promise of pervasive sensing. For example, the Jindo bridge wireless monitoring system cost under $200/channel (Jang *et al*. 2010).

Though extensive study has been conducted on the development and implementation of wireless sensors for short-term and long-term monitoring, very limited efforts have been made for seismic structural monitoring using wireless systems, due to some fundamental challenges. The first challenge is the constraint on power resources. Most conventional wireless sensors rely on batteries for power supply. Even if periodically recharged and replaced, the battery power source poses limits for always-on monitoring needed for detecting earthquakes, which can occur at any time. Therefore, duty-cycling is employed to preserve limited battery power for WSSs, waking them up periodically from deep sleep (Kim *et al*. 2007). While

*Corresponding author, Postdoc Research Associate, E-mail: fu303@purdue.edu
[a] Ph.D. Student
[b] Research Associate
[c] Professor
[d] Assistant Professor

ISSN: 1738-1584 (Print), 1738-1991 (Online)

suitable for periodic monitoring, duty-cycling is fundamentally incompatible with seismic monitoring; wireless sensors will miss the occurrence of earthquakes when they are in power-saving sleep mode. As a result, the MICAz nodes on the Golden Gate Bridge were unable to detect the three earthquakes that occurred during the three-month monitoring expedition (Cheng and Pakzad 2009).

To address the power constraint, one intuitive strategy is to use a sufficient power source, emulating traditional wired monitoring systems. Potenza *et al*. (2015) installed a network of 17 WSS on a historical church and employed the existing electrical lines to power the sensors for earthquake monitoring. The strategy did not retain the inherent advantages of cable removal for WSS, such as ease of installation and associated cost reduction. Likewise, Grillo (Wade 2019) developed a low-cost sensor, called Pulse. They leveraged Power over Ethernet (PoE) technique to provide energy for sensors and transmit data back to end users. It relies on the ethernet ports which are not available in many types of structures (e.g., bridges). Another strategy is event-triggered sensing, in which sensing is only initiated when events of interest are detected. Such techniques address the power constraint, which has the potential to enable seismic monitoring for universal types of structures. Hung *et al*. (2018) developed sensing nodes which were integrated with wake-on radios to periodically listen wake-up commands at ultralow power. On the other hand, a sentry node embedded with an earthquake early warning (EEW) system was always-on to detect P-waves and broadcast commands to wake up sensing nodes. Similarly, Fu *et al*. (2018a) developed a *demand-based WSS* by leveraging a trigger accelerometer. The sensor nodes woke up independently if the vibration is large, eliminating the sentry node that requires a complicated device (e.g., EEW) to further reduce the cost. The innovative work is initially focused on a single node; further exploration is highly desired for a network of WSS for seismic structural monitoring.

Another challenge is the limited network throughput, which makes it extremely difficult to support rapid condition assessment of civil infrastructure subjected to earthquakes. In seismic structural monitoring, a large network of wireless sensors is generally required to obtain a meaningful characterization of the structural response. The conventional approach to data acquisition for large sensor networks is centralized data acquisition, and it can take significant amount of time before condition assessment in seismic structural monitoring. Another approach is decentralized data acquisition, in which raw measurement data is processed on sensor nodes and only useful information is transmitted back to the base station. It expedites the data retrieval by reducing the transmission data size, but raw measurement data is not available for additional extensive processing (Cheng and Pakzad 2009).

Real-time data acquisition is an attractive approach herein, because it can eliminate delay for data transmission without sacrificing the information to be delivered (Linderman *et al*. 2013). However, due to constraints from operating systems (OS) and potential radio interference, real-time data acquisition is still a challenge for wireless smart sensor networks (WSSN). In particular, the widely adopted event-driven OS, such as TinyOS, in WSSNs has limited support for real-time applications, because the scheduler runs in a First-In-First-Out (FIFO) manner and uncertain delay of task executions is inevitable, resulting in potential scheduling conflicts. To avoid the conflicts, one intuitive way is to set sampling interval conservatively large, ensuring each step typically occurs within the time allotted (Linderman *et al*. 2013). However, the throughput of each WSS is thus reduced significantly. Alternatively, an OS with multithreading support was developed (Lynch *et al*. 2006, Wang *et al*. 2007), in which interrupts preempted any non-real-time task to service the software routine associated with the sensing process to ensure a precise schedule without delay. The system was estimated to achieve near-synchronized 16-bit data acquisition of up to 24 sensor channels at a sampling rate of 50Hz in real-time. This has yet to be validated in testing.

In addition to the OS constraints discussed in previous paragraph, interference-free data transmission in a WSSN is also challenging for real-time data acquisition. To address it, each node must be scheduled carefully, by utilizing code-division multiple access (Han *et al*. 2012), frequency-division multiple access (Chen and Casciati 2014), or time-division multiple access (TDMA) (Niu *et al*. 2009, Whelan and Janoyan 2009, Linderman *et al*. 2013). Among these strategies, TDMA is the most popular strategy for real-time applications. Based on transmission scheduling, the system developed by Whelan and Janoyan (2009) was validated to support real-time data acquisition of 12-bit 40 channels at a sampling rate of 128 Hz. The scheduling of transmission is based on time synchronization, which is however only precisely maintained for the initial several minutes. After comprehensive timing analysis, Linderman *et al*. (2013) proposed a staggered TDMA and implemented it on Imote2s to enable high-throughput, real-time data acquisition of 12 channels at 40 Hz sampling rate. The framework was based on TinyOS, which imposed limits for throughput of less than 50 kbps. In sum, high-throughput real-time data acquisition is still challenging for WSSN.

To address the aforementioned challenges, this paper presents the development of *xShake*, a wireless seismic monitoring system for civil infrastructure. Built upon the authors' previous research on sensor development, it employs event-triggered wireless sensor prototypes, which initiate sensing only in response to seismic events, overcoming the energy constraints. Moreover, it is equipped with a live-streaming framework, achieving high-throughput, real-time data acquisition. In addition, a rapid condition assessment application is developed on the basis of MATLAB to process and visualize measurement data in real-time for end users. The main contribution of this study is the development of the live-streaming framework and the rapid condition assessment application; furthermore, the integrated system, involving the co-design of hardware, software, and signal processing, addresses the main challenges of wireless seismic monitoring of civil infrastructure. Lab tests were carried out to demonstrate that, the developed system can capture high-fidelity synchronized data under earthquakes and enable real-time

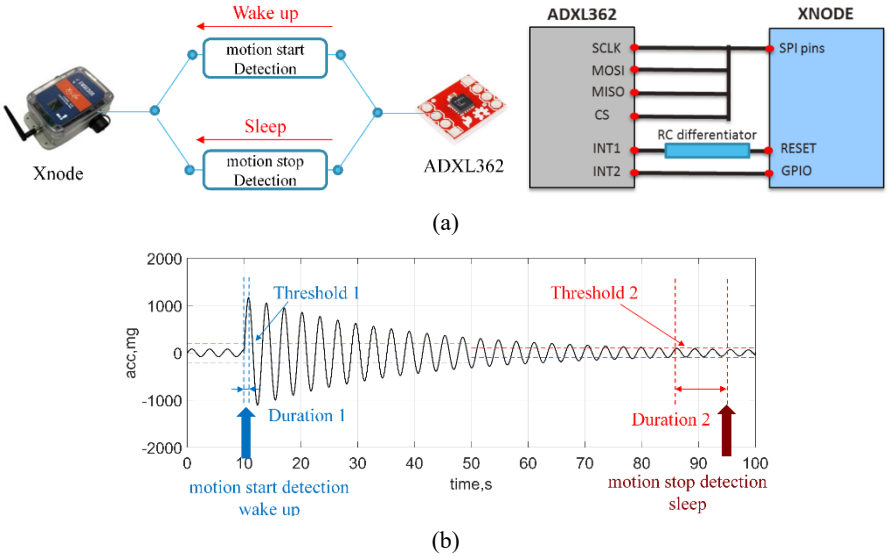

Fig. 1 First-generation prototype: (a) communication between trigger sensor & Xnode; (b) event detection concept

structural condition assessment.

2. Wireless sensor prototypes for on-demand sensing

The first challenge regarding wireless seismic structural monitoring is the power constraint. In particular, wireless sensors must maintain always-on monitoring, so as not to miss an earthquake, under a minimal power budget, without sacrificing data fidelity. To address this challenge, the *demand-based WSS* developed by the authors (Fu *et al*. 2018a, b) is applied herein for seismic structural monitoring. A brief overview about the development of sensor prototypes is provided in this section, which consist of two generations. The first generation enables event-triggered sensing similar to commercial counterparts; the second generation advances the prototype with two unique features: switch circuits to minimize power consumption and data fusion to avoid data loss. Note that, similar on-demand sensing technologies have been developed for general purpose monitoring (Sutton *et al*. 2017, Popovic *et al*. 2017, Liu *et al*. 2018), but most of them are not applicable for seismic structural monitoring, either due to their low-fidelity data acquisition or high risk of data loss, detailed in the paper (Fu *et al*. 2018a).

2.1 First-generation prototype

The first-generation prototype aims to realize the basic functionality of event-triggered sensing in two aspects: 1) detecting the occurrence of events (e.g., earthquakes) and starting high-fidelity sensing immediately; 2) detecting the end of events and interrupting sensing to save energy without missing any part of event-induced vibrations. It consists of two key components: an ultralow-power trigger accelerometer to continuously monitor structural vibration, and a sensor platform to obtain high-fidelity measurement data and host computation intensive applications. Among the trigger sensors in the market, the ADXL362 is selected, because of its low power consumption, high-quality sensing characteristics, and large buffer to record measurement data surrounding the onset of events. On the other hand, the Xnode Smart Sensor, developed by Embedor Technologies, is chosen for the host sensor platform (Spencer *et al*. 2016). It features high sensing resolution, high sampling rate, powerful microprocessor, and open-source application software (Fu *et al*. 2019).

The integration of two components is illustrated in Fig. 1, enabling event-triggered sensing. Particularly, when the vibration exceeds a user-defined value (threshold 1) over a period of time (duration 1), indicating an event (e.g., earthquake) starts, the trigger sensor can wake up the host sensor platform to start high-fidelity sensing. When the vibration is below another user-defined value (threshold 2) over a period of time (duration 2), indicating the event stops, the trigger sensor can interrupt the sensing process and make the sensor platform sleep again. To achieve the integration, proper circuits are designed to enable three functionalities: (i) communicating commands/data between the ADXL362 and the Xnode, (ii) waking up the Xnode from deep sleep mode when an event starts, and (iii) interrupting sensing process when the event stops. In addition to hardware development of the prototype, an effective application framework is developed using the open-source software of Xnodes, to control the behavior of both the ADXL362 and the Xnode to enable event-triggered sensing.

Though the functionality of event-triggered sensing is realized, the current draw of the first-generation prototype is 10.2 mA, when the host sensor platform is in deep sleep mode. It is worthwhile to clarify that the Xnode itself consumes a small amount of power in sleep mode, but in the prototype, in order to maintain the continuous operation of the trigger sensor, the microcontroller unit of the Xnode is still kept running, albeit at an ultra-low clock rate. This consumes more power than expected. Such high current draw cannot sufficiently address the constraints in power

resource. If a single lithium-polymer battery of 10,000 mAh is used, the proposed prototype can only support always-on monitoring for up to one month. Therefore, an improved version of the sensing prototype is desired to further reduce the power consumption.

2.2 Second-generation prototype

Similar to the first-generation prototype, the second-generation prototype consists of an ultralow-power trigger accelerometer and a high-fidelity sensor platform. The unique feature of the new prototype is that, it employs the trigger sensor as the virtual switch that can fully power off the platform when no event occurs, minimizing the power consumption from mA level to μA level. In particular, the switch isolates the power supply of the trigger sensor from the Xnode, such that the Xnode can be totally powered off whilst the trigger sensor can continue sensing in ultra-low power mode.

As shown in Fig. 2, to realize its unique feature, a programmable event-based switch was designed and implemented on the radio/power board of the Xnode in the *demand-based WSS*. A trigger accelerometer (ADXL362) and a real time clock (DS3231M) are included to control the state of a MOSFET; hence, they can both enable/disable the power supply of the Xnode, acting as a virtual switch. An AND gate and a Latch circuit are added to maintain the output signals from the ADXL362 and the DS3231M. The triggering conditions for the ADXL362 and the DS3231M can be reprogrammed by the microcontroller unit through SPI and I2C communication protocols, respectively. When the vibration exceeds a user-defined threshold, the triggering signal generated by the ADXL362 flips the state of the MOSFET, turning on the Xnode and initiating high-fidelity sensing. When the event ends, another triggering signal from the ADXL362 notifies the Xnode to stop high-fidelity sensing and power off afterwards by flipping the MOSFET state. In addition to the trigger sensor, the real-time clock supports the nodes operating in duty-cycles, retaining traditional functionality for periodic monitoring. Particularly, the clock sends a triggering signal periodically to flip the MOSFET state and turn on the Xnode. The nodes remain awake and listen to messages from the base station. Because of the virtual switch, the new generation prototype achieves a current draw of only 365 μA when no events occur. It extends the lifetime of always-on monitoring to over three years using a single lithium battery. This feature helps to successfully detect the occurrence of earthquakes with minimal power budget in long-term monitoring.

Another important functionality of the new-generation prototype is post-sensing data fusion to avoid data loss. Generally, response times of wireless sensors from a cold boot to full-bore data acquisition are typically around one second, due to system boot-up process, sensor initialization and warm-up, and filtering delays. As a result, the critical data surrounding the onset of earthquakes will be lost, typically well over a second. To avoid this data loss, on-board post-sensing data fusion is proposed (Fig. 2(c)). Specifically, the ADXL362 data is first upsampled to the same sampling rate with Xnode data. The last portion of ADXL362 data is synchronized with the first portion of Xnode data by maximizing their cross-correlation value. The RMSE and the optimal offset of overlapping data in the ADXL362 and that in the Xnode are obtained. Because the ADXL362 data may not have accurate sampling rate, it should be resampled with a slightly different sampling rate (ranging from 0.9 kHz to 1.1 kHz) and then processed with the same step to obtain the corresponding RMSE value. The sampling rate that is corresponding to the minimal RMSE is selected to calibrate the entire ADXL362 data, and corresponding offset is used to synchronize ADXL362 data and Xnode data, and eventually, they are fused to produce a complete representation of the acceleration record. More details can be found in the paper (Fu *et al*. 2018a).

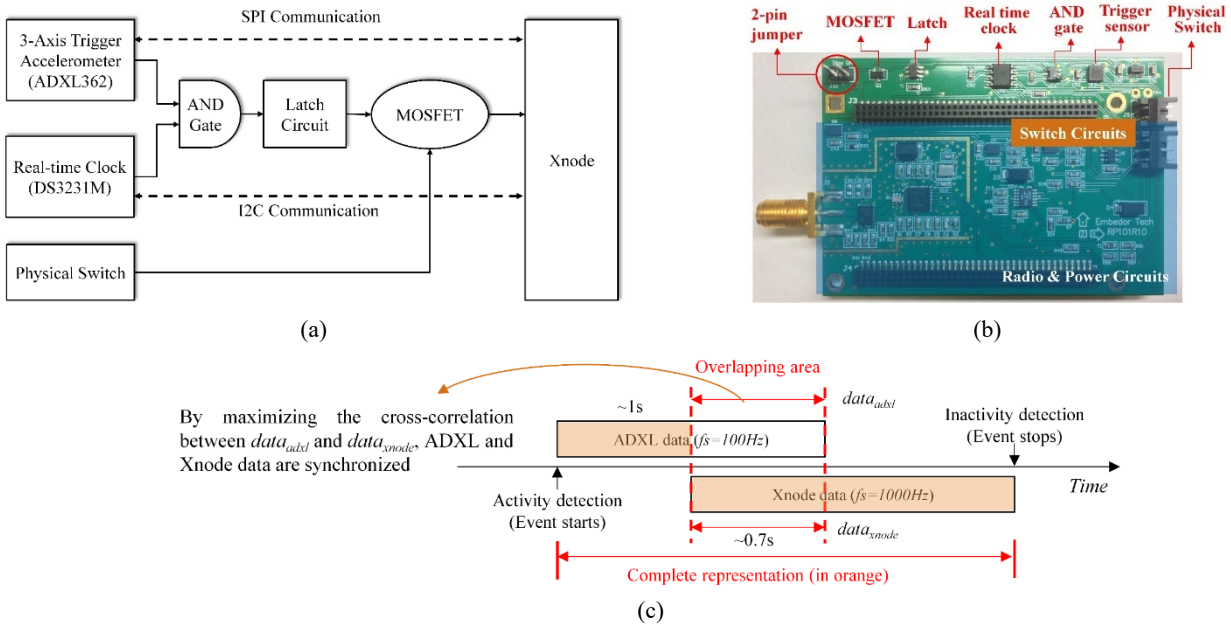

Fig. 2 Second-generation prototype: (a) functional block diagram; (b) realized PCB; (c) data fusion

Table 1 Comparison of on-demand sensing prototypes for SHM

Prototypes	Study	A/D (bit)	Sampling rate (Hz)	Channels	Power usage (mW)*	Data loss compensation
TelosW	Lu *et al*. (2010)	13	100^{+}	3	10.5	No
Low-power WSSN	Torfs *et al*. (2013)	13	200^{+}	3	0.4	Yes
Sentinel-based WSN	Popvic *et al*. (2017)	24	123^{+}	1	0.0006	Yes$^{\times}$
EEW-based WSN	Hung *et al*. (2018)	16	N/A	3	1.1	Yes
EcoVibe	Liu *et al*. (2018)	14	N/A	3	0.00012	No
Demand-based WSS	Fu *et al*. (2018)	**24**	**1000**	**8**	**1.1**	**Yes**

*power consumption during no event is compared here, which is critical for power constraints.
$^{+}$ the maximum available sampling rate reported in the literature is collected.
$^{++}$ estimated value based on paper's results is listed.
$^{\times}$ the compensation strategy is not applicable for seismic SHM.

In sum, *demand-based WSS*s address the power constraint of seismic monitoring of civil infrastructure, detecting earthquakes with minimal response latency and without sacrificing high-fidelity measurements. Second-generation prototypes are considered herein for seismic structural monitoring, because of its low power consumption and data fusion technique. Table 1 summarizes the pros and cons between the selected prototype (in bold) with other existing methods for on-demand sensing. As can be seen, the *demand-based WSS* has the best performance for high-fidelity SHM, with respect to A/D resolution, sampling rate and channel number, suitable for seismic structural monitoring. Particularly, our prototype has three channels reserved for triaxial accelerations and five channels are left available for user-configurable external analog sensors. It also has satisfactory power efficiency, enabling long-term monitoring for unpredictable earthquake events. In addition, its post-sensing data fusion compensates the initial data loss due to cold booting, applicable for seismic SHM. The application performance and validation of *demand-based WSS* will be discussed in Section 5.

3. Live-streaming framework

The second challenge regarding wireless seismic monitoring is the limited network throughput. Specifically, a WSSN should transmit back the measurement data in an efficient manner, without interference between nodes, so as to support rapid structure assessment under earthquakes. To address this challenge, an efficient live-streaming framework is developed to support high-throughput real-time data acquisition for WSSN. In particular, preemptive multitasking is implemented to address the scheduling conflicts between sensing and radio transmission in each sensor node, and adaptive Time Division Multiple Access (TDMA) is developed to minimize the radio inference between multiple sensor nodes for lossless data transmission over long-duration measurement.

3.1 Preemptive multitasking implementation

Event-driven operating systems (e.g., TinyOS) employed in many wireless sensors impose the limits for the real-time data acquisition of WSSNs. Particularly, tasks are executed in FIFO manner in the event-driven OS. Hence, real-time data acquisition is difficult to realize, because critical tasks (e.g., sensing operation) may be delayed by execution of preceding tasks (e.g., data transmission), given that non-deterministic delays in task execution are inevitable. The task delay of FIFO tasking depends on the hardware and the operating system. A typical example is the Imote2. Based on the timing analysis of sensing process (Linderman *et al*. 2013), up to 300 μs delay is observed for data processing task in sensor nodes and up to 800 μs delay is observed in the gateway side. As a result, such constraints from the OS make it extremely difficult to address the scheduling conflicts between current tasks, imposing the limits of achieving high-throughput real-time data acquisition. Although some studies have been made to mitigate the scheduling conflicts by conducting timing analysis (Linderman *et al*. 2013), maximum sampling rate has to be reduced.

To address the issue, preemptive multitasking is considered in developing the live-streaming framework. Using preemptive multitasking, tasks are well-organized with different priorities and managed by a scheduler at run time (Fu *et al*. 2016). Tasks with lower priorities are preempted by important tasks, resolving the scheduling conflicts between critical tasks and other tasks. Its cost of a small processing overhead is an acceptable trade-off for powerful sensor platforms such as Xnodes and Imote2s. The benefit of applying preemptive multitasking is illustrated in Fig. 3. For the sake of comparison between two scheduling schemes, the live-streaming framework is simplified to contain only three typical tasks: sensing, transmitting, and processing. As it is shown, the transmitting task is suspended and gives way to sensing task, when scheduling conflict occurs. Therefore, the delay of sensing is prevented in real-time data acquisition, ensuring the precision of sensing without compromising the throughput within a single node.

The detailed structure of real-time data acquisition in preemptive multitasking framework is shown in Fig. 4. Four tasks are defined for each sensor node, including Application Task, Receiving Task, DataSend Task, and Sensing Task. They are assigned with different priorities based on their latency tolerance. In particular, the

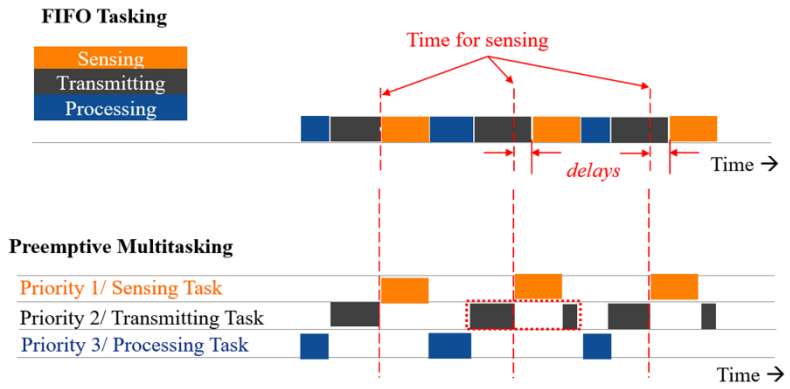

Fig. 3 Comparison of the two scheduling schemes: FIFO tasking & preemptive multitasking

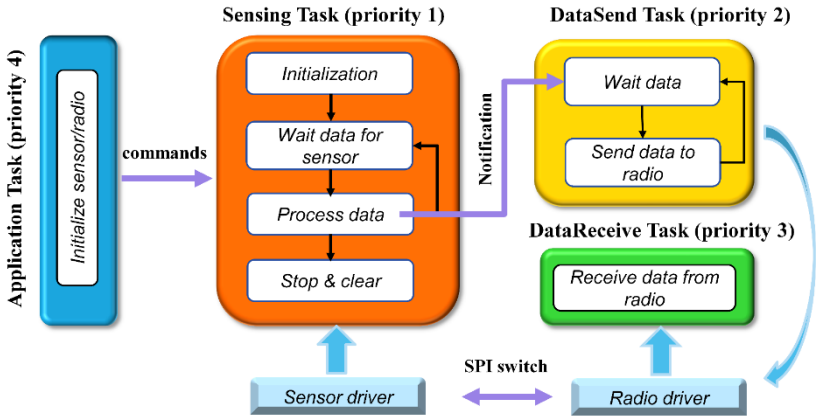

Fig. 4 Detailed structure of real-time data acquisition in preemptive multitasking

Application Task is utilized to initiate the operation of sensor nodes and monitor the behavior of other tasks. If an unexpected lock-up occurs, the task will reset the node. A large delay is acceptable for these operations, so the task priority is the lowest in the application. The Sensing Task manages the data collection process from sensors to measure structural response. It has the highest priority, because large delays of this task will result in loss of measurement data. The DataSend Task, with lower priority, is aimed to send the data which has been processed in the Sensing Task. The transmission time of a single data packet is actually larger than the sampling interval of raw data in the Xnode. Instead of splitting transmission operation carefully among multiple sampling intervals if using TinyOS (Linderman *et al*. 2013), preemptive multitasking can avoid the interruption of the sensing process with reduced programming efforts and more efficient usage of the time schedule. The Receiving Task with a lower priority is defined to receive potential messages or commands from the base station. In addition, another conflict is involved in low-level drivers for sensing operation and radio transmission. More precisely, the radio driver and sensor driver share the same Serial Peripheral Interface (SPI) bus, when they handle interrupts during real-time data acquisition. To resolve the potential SPI conflicts, a mutual exclusion primitive is utilized to coordinate the sensor driver and radio driver, ensuring that each SPI access is atomic.

3.2 Adaptive time-division multiple access protocol

To allow multiple sensor nodes to transmit data back to the base station in real time, radio interference should be avoided between sensor nodes. As a common strategy, TDMA is considered herein. Basically, sensor nodes are allocated with different time slots to transmit measurement data, such that only one sensor node can transmit data at a time. As a result, the radio interference is minimized, and high packet reception rate can be achieved. To increase the throughput, Linderman *et al*. (2013) developed the staggered TDMA scheme. Particularly, multiple samples are buffered in a single packet and transmitted at the same time. Though the latency is increased, the efficiency of data transmission is improved, and the throughput is significantly expanded.

However, the staggered TDMA scheme is a poor fit for seismic structural monitoring. Particularly, to support the schedule, precise time synchronization between multiple sensor nodes is required. To this end, a 30-s time synchronization phase is carried out prior to sensing in the staggered TDMA, a.k.a., pre-sensing time synchronization (Nagayama and Spencer 2007). It is mainly because the aforementioned constraints in event-driven OS make it extremely difficult to conduct time synchronization during sensing, and long-duration beacons exchange is required to estimate the clock drift precisely. As a result, a long delay is introduced for measurement, and data loss of seismic

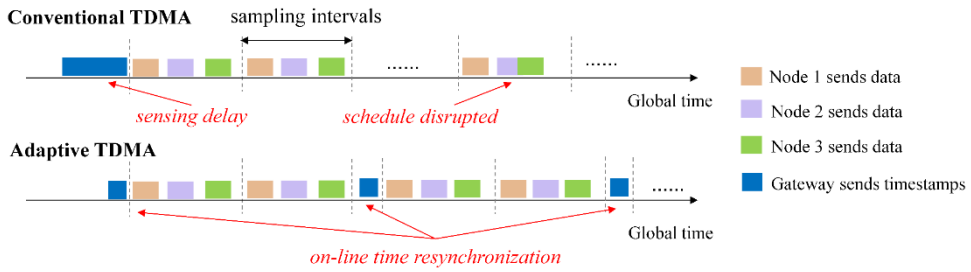

Fig. 5 Comparison of two TDMA scheduling schemes: Conventional TDMA & Adaptive TDMA

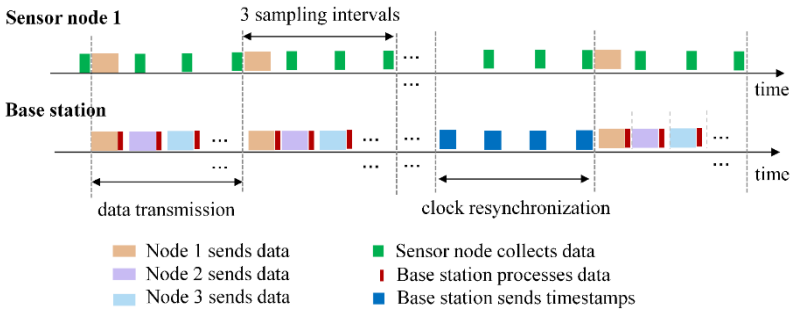

Fig. 6 Detailed time scheduling for adaptive staggered TDMA protocol

monitoring becomes serious. On the other hand, the one-shot time synchronization is only viable for several minutes, after which the TDMA schedule is disrupted by clock drift effect and the likelihood of radio interference becomes more serious over long-duration measurement.

To address the challenges of using TDMA, a new adaptive strategy is designed for real-time data acquisition by utilizing a preemptive multitasking scheme (Fig. 5). More specifically, a new task is created to handle time synchronization during the sensing process, without introducing scheduling conflicts. The task is triggered periodically by a timer using semaphores. Accordingly, the local clock in each node is not only synchronized prior to sensing, but also resynchronized periodically. During clock resynchronization, the base station broadcasts multiple timestamping beacons to sensor nodes. While receiving the beacons, sensor nodes stop data transmission but continue sensing process. In the meantime, the clock drift and offset are estimated and compensated in each sensor node, and the staggered TDMA schedule is stable over long sending period. Moreover, because of resynchronization, initial time synchronization prior to sensing can be reduced from 30 s to less than 1 s, and the sensing delay is minimized.

Fig. 6 shows the adaptive scheduling scheme implemented for seismic monitoring of civil infrastructure. In each sensor node, data transmission is fully independent of sensing process and is scheduled by every three-sampling interval. During the interval, sensor nodes collect data during sensing process, buffer three samples into a single packet, and send it at the designated time slot. Every 60 seconds, sensor nodes stop transmission and receive beacons from the base station. On the other hand, the gateway node receives data packets from sensor nodes and processes them afterwards. Every 1 minute, the gateway node stops receiving packets and broadcasts timestamping beacons. As it can be shown, because of stable and precise clock synchronization, the three-sampling interval can be made full use of for transmission without worrying radio interference between different nodes. A lab test is later conducted to evaluate the proposed strategy. The result shows that it can support up to 36 sensing channels with a sampling rate of 100 Hz without packet loss, corresponding to 115.2 kbps.

To demonstrate the performance of adaptive TDMA, multiple repeated lab tests were conducted involving one gateway node and three sensor nodes, sampling at 200 Hz. Both conventional TDMA and adaptive TDMA are implemented, in both of which three samples are buffered in a single packet, following the paper (Linderman *et al.* 2013). The real-time data acquisition has been repeated a least five times each for three different sensing durations: 1 minute, 3 minutes, and 5 minutes. The package reception rate (PRR), which serves as a performance indicator to quantify data loss, is averaged for the repeated tests, and

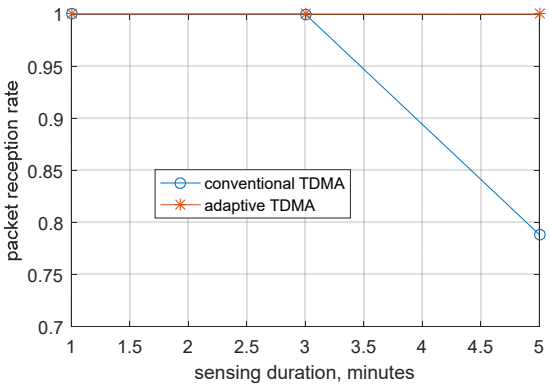

Fig. 7 Performance comparison of two TDMA

plotted in Fig. 7. It can be found that the PRR is very close to 100%, for conventional TDMA if the sensing duration is less than 3 minutes, but it is reduced to 78% for 5 minutes real-time data acquisition. However, the PRR is always close to 100% for adaptive TDMA for all the tests, demonstrating that it outperforms the conventional TDMA for long-duration measurement.

In addition, the periodic update of clock drift estimation is further used to support high-precision real-time time synchronization of sensing data. As shown in Fig. 8, before sensing starts, one round of point synchronization is carried out to synchronize the local clock among sensor nodes. During sensing process, the clock drift is compensated piece-wisely in each sensor node, and the clock offset for samples is estimated and recorded alongside in each packet. In the gateway node, upon receival of packets, data synchronization is carried out periodically to obtain the synchronized measurement. The process continues until the event stops. The test results show that, the implemented real-time time synchronization strategy can achieve high-precision synchronized sensing with an error of less than 20 μs. The details of time synchronization strategy for real-time data acquisition can be found in the paper (Fu *et al.* 2020).

The performance of the proposed live-streaming framework is tested in the lab and then compared with other real-time data acquisition schemes obtained in the literature, as summarized in Table 2. Because of resolving scheduling conflicts using preemptive multitasking, the maximum sampling rate of a single node can be increased to 500 Hz. Meanwhile, the network of wireless smart sensors can achieve the throughput of 115.2 kbps. It should be clarified that, if the sensor node is configured with highest sampling rate (500 Hz), the network can only support a single node for real-time data acquisition. In addition, the adaptive TDMA schedule extends the prescribed transmission schedule to around half an hour, with time synchronization error of less than 20 μs; it also minimizes the time for synchronization prior to sensing, addressing the concern of initial data loss. It is worthwhile to mention that, because of two constraints in WSS (i.e., scheduling conflicts within each sensor node and the radio interference between multiple nodes), the highest configuration of the Xnode may not be achieved. But the proposed framework alleviates both constraints and helps to achieve high-throughput seismic monitoring of civil infrastructure in real-time.

Table 2 Comparison between proposed strategy with wireless real-time data acquisition schemes

Study	Max rate (Hz)	Throughput (kbps)	Scheduled time (min)	Time before sensing (s)	Time sync error (μs)
Wang *et al.* (2007)	50*	26	<6	<1	20
Niu *et al.* (2009)	50*	17	N/A	N/A	N/A
Whelan and Janoyan (2009)	128*	61.4	4~5	<1	N/A
Linderman *et al.* (2013)	115	46	several	~30	<80
Xiao *et al.* (2017)	200*	86.4-	N/A	5+	21.57+
Proposed framework	**500**	**115.2**	>25	**<1**	**<20**

*the maximum available sampling rate reported in the literature is collected.
- the throughput is derived by the authors based on the data in the paper.
+ the synchronization error is found in the paper (Xiao *et al.* 2012), and it is clock synchronization.

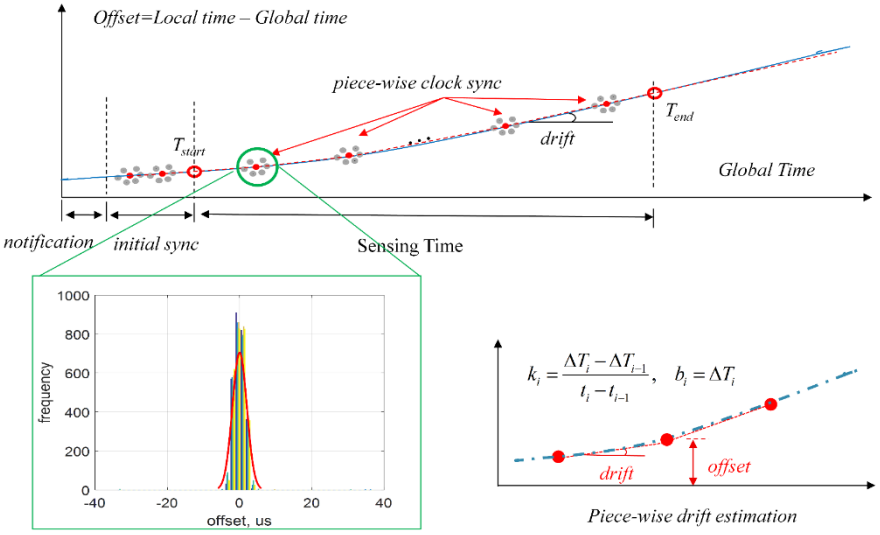

Fig. 8 Real-time time synchronization flowchart in sensor nodes

4. Rapid condition assessment application

The proposed monitoring system has advantages over existing frameworks in two aspects: 1) the sensing prototype has higher ADC resolution, higher sampling rate, larger channel number, and data loss compensation. As a result, it can help to provide high-fidelity high-rate multi-channel seismic monitoring data from each sensor node. 2) the live-streaming framework has higher throughput, higher allowable sampling rate, lower synchronization error, and longer stable measurement duration. As a result, it can help to support large-scale sensor network over long-duration real-time monitoring. In sum, the benefits in the above aspects can improve the accuracy of condition assessment and expand the monitoring area of more complex structures through densely deployed sensor networks. To fully realize rapid condition assessment, a MATLAB-based application is developed, which consists of two main parts: 1) code performing online condition assessment, and 2) a graphical user interface (GUI) to allow end-users to interact with the wireless monitoring systems and enable real-time data visualization. The details of the application are presented in this section.

Interstory drift is widely recognized as an important quantity to assess building performance and damage during earthquakes. Therefore, interstory drift estimation using acceleration record is implemented in the application, as illustrated in Fig. 9. Particularly, time-synchronized acceleration digital records with the same sampling frequency at two consecutive floors are used to obtain relative acceleration, Δa, which is processed through a finite impulse response (FIR) filter designed for the structure, and finally interstory drift estimation is obtained. The role of FIR filter is to perform double integration and high pass filtering simultaneously, following the idea of displacement estimation using acceleration records (Gomez *et al*. 2018). Specifically, the FIR filter can be represented by a vector of coefficients **c** of length $2k + 1$; the coefficients are given by

$$c_{p+k+1} = -\frac{f_s}{2\pi^2}\int_0^{f_s/2} \frac{f^{2n-2}}{f^{2n} + \lambda^{2n} {f_T}^{2n}} \cos(2\pi p f \Delta t)\, df \quad (1)$$

where k is determined by the normalized window length N_w, the target frequency f_T, and the sampling frequency f_s

$$k = N_w \frac{f_s}{2f_T} \quad (2)$$

Utilizing the filter coefficients, the estimated displacement is expressed as

$$u_i(t) = (\Delta t)^2 \sum_{p=-k}^{k} c_{k+1+p} a_i(t + p\Delta t) \quad (3)$$

where $u_i(t)$ is the deformation of i^{th} floor at time t, $a_i(t)$ is the associated acceleration, and Δt is the sampling time. Note that the vector of coefficients is the same for i^{th} floor and $i+1^{th}$ floor, because they are part of the same structure and the records have the same sampling frequency. Accordingly, the interstory drift $\theta_i(t)$ is given by the difference of deformations between two adjacent floors

$$\begin{aligned} \theta_i(t) &= u_{i+1}(t) - u_i(t) \\ &= (\Delta t)^2 \sum_{p=-k}^{k} c_{k+1+p}[a_{i+1}(t + p\Delta t) - a_i(t + p\Delta t)] \end{aligned} \quad (4)$$

The detailed design of FIR filter can refer to the paper (Gomez *et al*. 2018). Following the conventional criteria (Celebi 2013), if the interstory drift ratio exceeds 0.2%, the corresponding story has minor damage; if the drift ratio is larger than 0.8%, the story is severely damaged. The story height is generally around 10 feet (3 m), so the absolute drift should be larger than 0.24 inch (6 mm) for the first threshold and larger than 0.96 inch (24 mm) for the second threshold. With this, the application can assess building conditions in real-time under earthquakes. It is worthwhile to clarify that the main objective of this strategy is to enable rapid damage assessment. If the drift ratio exceeds the threshold in a certain floor, engineers can be notified immediately about "potential damage" and prepare for a more thorough inspection. False positive scenarios could happen, but should not be of critical significance.

In addition, a GUI is designed herein, as shown in Fig. 10. It contains four components: (1) a control panel for inspectors to configure the proposed system, (2) a notification bar to show the status of the system, (3) a condition summary table to present early damage assessment results, and (4) multichannel measurement display for real-time visualization of measurement data. While sensor nodes are sensing, data samples are collected and transmitted continuously by the base station. In the meantime, the GUI plots the measurement history data in real-time. In the current configuration, the GUI can support six channels' data visualization for either acceleration measurement, or displacement estimation. Note that because of the intrinsic filter latency, a delay of approximate 2 s exists between acquisition and animation plotting. With the GUI's help, users can see the time history of structural vibration during earthquakes and understand the structural behavior in real-time.

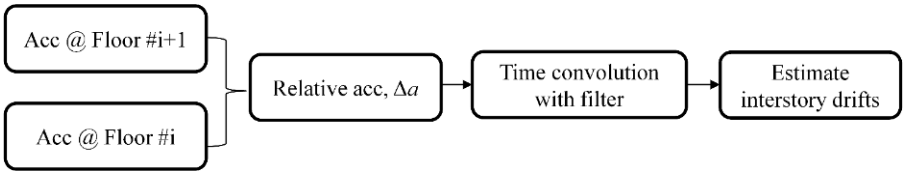

Fig. 9 Flowchart of rapid condition assessment of buildings

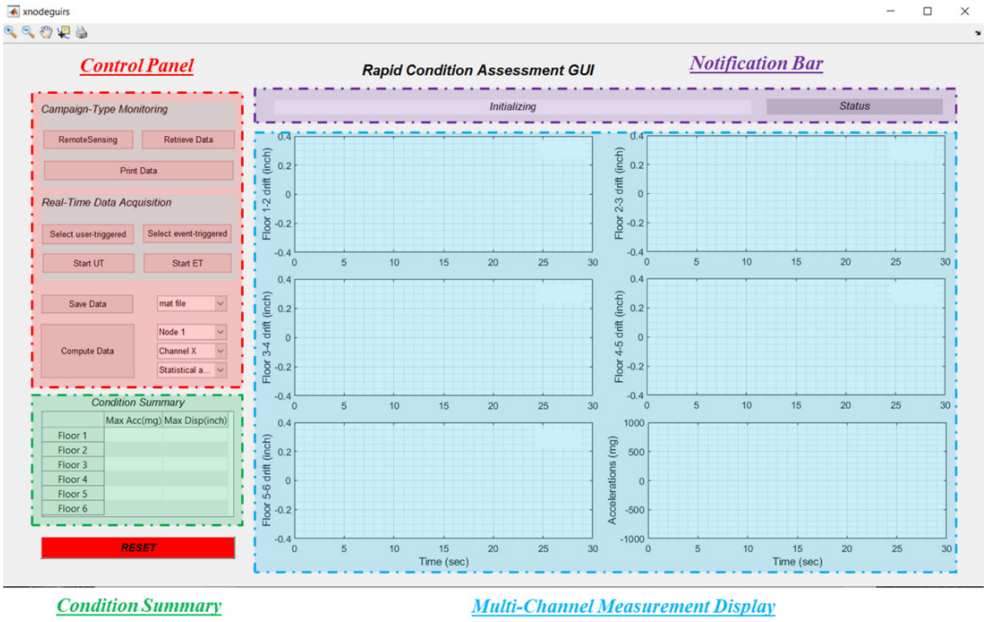

Fig. 10 Graphical user interface of the efficient data management application

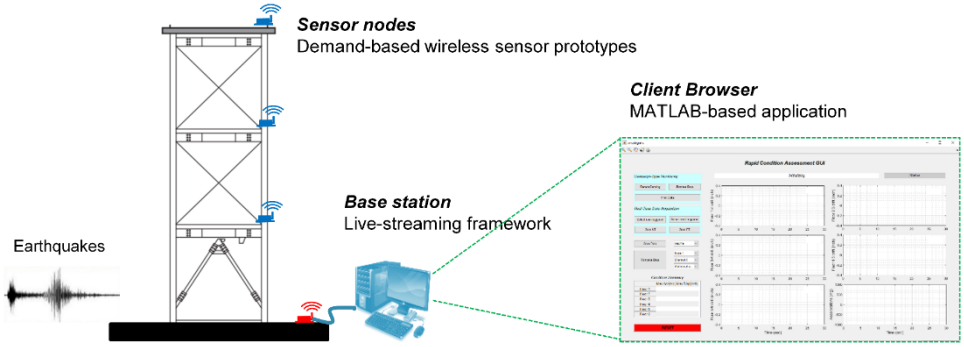

Fig. 11 Deployment concept of *xShake* for building monitoring

5. Performance evaluation of *xShake*: seismic building monitoring

To validate the performance of the *xShake*, a laboratory test was carried out for seismic building monitoring. This section describes the deployment concept of the integrated system, experimental setup, and results discussion.

5.1 Deployment concept

Fig. 11 shows the deployment concept of the integrated seismic monitoring system, which consists of multiple sensor nodes, a base station, and a client browser. The aforementioned three components that developed in this study sit in each of three parts, respectively. The demand-based wireless sensor prototypes are in deep sleep mode most time to save battery energy, utilizing solar panel for power harvesting to prolong their lifetime over years. When an earthquake occurs, the sensor nodes wake up and start sensing immediately; when the earthquake stops, they stop measurement automatically. In the meantime, the nodes record the time when the earthquake occurs, in the form of 24-hour clock and Gregorian calendar. On the other hand, the base station is always on, powered on by wall power, waiting for the notification message of events from sensor nodes. Once the notification is received, the base station coordinates sensor nodes to perform real-time data acquisition based on the live-streaming framework. During the live streaming, the collected data samples are synchronized in the base station by real-time time synchronization. Meanwhile, the client browser reads measurement data from the base station and conducts online condition assessments. Both measurement data and condition results are visualized in real-time.

5.2 Experimental setup

In the lab test, a 6-story building model was instrumented with the *xShake* system (Fig. 12). It was mounted on a uniaxial shaking table. The shaking table can simulate earthquakes in one horizontal direction, driving a 15 kg mass at 2.5 g with a maximum stroke of ±7.5 cm. The Kobe earthquake excitation was generated by the shaking table to represent a seismic motion for the building structure. Six wireless sensor prototypes were installed on each floor of the building model. The onset of a seismic

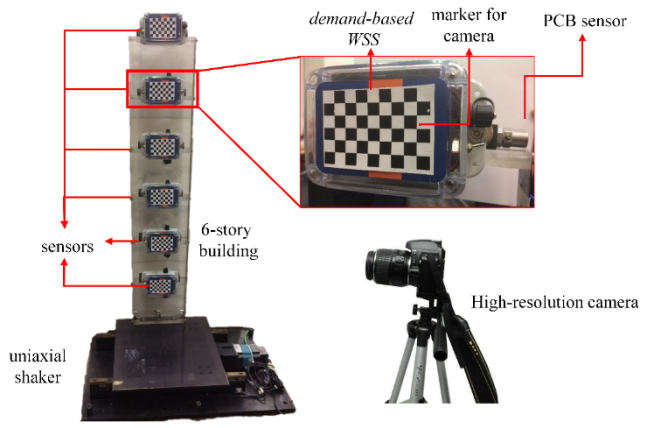

Fig. 12 Test setup for seismic building monitoring

motion was detected when the structural vibration was above 80 mg for over 0.02 s; sensor nodes immediately woke up and notified the base station. Afterwards, the base station broadcasted sensing parameters and beacons containing global timestamps for initial time synchronization. Then sensor nodes started real-time data acquisition and conducted high-quality sensing at 100 Hz. The rapid condition assessment application collected data from the base station and performed interstory drift estimation in real-time. In the meantime, plots 1-5 in the GUI showed the plot of interstory drift estimations in real-time. In addition, plot 6 in the GUI showed the acceleration measurement from all of 6 floors. As a demonstration of rapid floor assessment, if the drift exceeded 5 mm during the earthquake, the animation line of associated interstory drift turned red. Note that the stiffness of each floor in the building model was very small, the threshold set in the test is much larger than the value used for real structures. The end of the earthquake was detected when the vibration was below 40 mg over 5 s; sensor nodes stopped measurement and reentered deep sleep mode. Accordingly, the application stopped animation line plotting and presented a summary of structural conditions, including maximum acceleration and displacement of each floor.

As a reference for comparison, displacements were obtained using vision-based measurements. Each sensor node had a checkerboard pattern visible to the camera as target using for tracking. The size of the pattern was 6-by-9, and the MATLAB toolbox for detecting and tracking of checkerboard pattern was used directly. Nikon D3300 camera with 18-55 mm lens were used, and data acquisition (video recording) was set to 60 frame-per-second (fps). In addition, wired piezoelectric accelerometers, model PCB353B33, were installed on the same floors. A dynamic signal analyzer, VibPilot, (m+p international) was employed as a data acquisition system for the wired sensors. The available sampling rates at the VibPilot should be powers of 2, and the value that is closest to 100 is 128. Therefore, the wired sensors were sampled at a frequency of 128 Hz. The measurement from wired sensors served as reference for acceleration comparison.

5.3 Results and discussion

During the test, the *xShake* successfully captured the seismic motion and provided early estimation of story conditions in real-time. Fig. 13 shows the screen capture of the GUI, in which structural responses are successfully captured, and interstory drifts between adjacent floors are estimated and plotted. The plot of Floor #3 drift is red, indicating the drift exceeding the threshold has occurred in this floor. Except for Floor #3, other floors are considered as intact. In addition, the structural responses are summarized on the bottom left of the GUI, as listed in Table 3 for details. The structure response at Floor #2 is relatively larger than other floors, with the maximum acceleration of 528.42 mg. As the number of floor increases, the displacement becomes larger. The top floor has the maximum displacement of 27.4 mm.

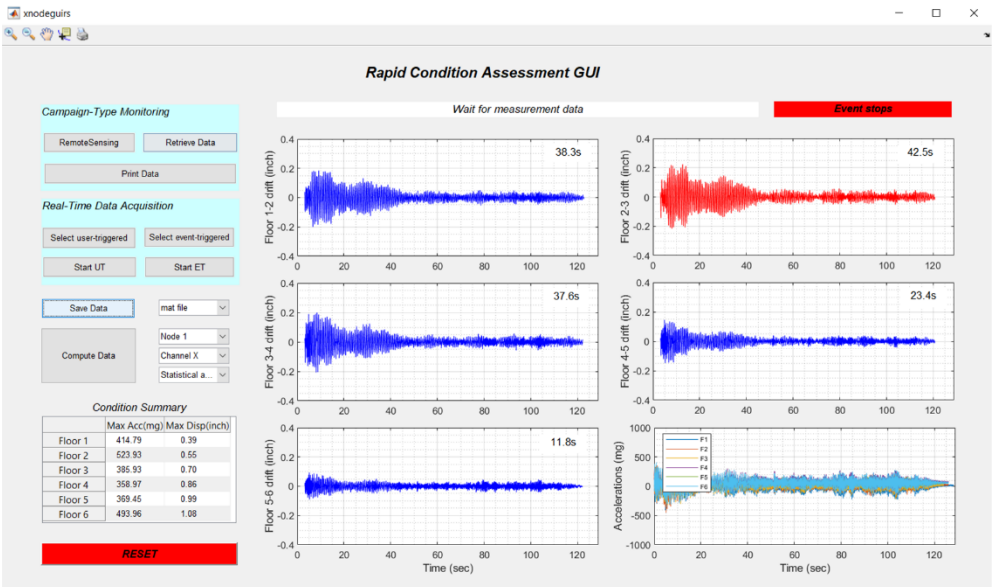

Fig. 13 Screen capture of rapid condition assessment GUI

To validate the measurement data from the *xShake*, the acceleration measurement data from wired sensors is compared with wireless sensor data. To make a direct comparison in the time domain, the data sets from wired sensors were downsampled to the same sampling rate as wireless sensor data. In addition, for fair comparison, both wired and wireless sensor data should have the same frequency bandwidth. Therefore, both wired and wireless sensor data were sent through an 8-pole elliptic low-pass filter with a cutoff frequency of 40 Hz. Finally, the wired sensor data sets were synchronized with the wireless sensor data by maximizing the correlation function between records. Fig. 14 shows the comparison of measurement data between the two monitoring systems in Floor #1, #3, and #5, respectively, in both time and frequency domain. The excellent agreement demonstrates the ability of the *xShake* to measure high-quality synchronized accelerations under seismic motions. Fig. 15 shows a time-window of comparison of the interstory drift estimation from Floor #2 to Floor #6 against the camera-based total interstory drifts. As these figures show, the estimated drift value and the reference values agree well for all time steps. In addition, Table 4 summarizes the comparison of both acceleration measurement and interstory drift estimation between the proposed system data and the reference system data. In particular, the root means square error normalized by the standard deviation of the reference data, NRMSE, is employed as the quantitative indicator. The lab test results in this section demonstrate the ability of the *xShake* to detect the occurrence of earthquakes, provide high-quality synchronized data, and present rapid condition assessment and real-time data visualization for inspectors.

Table 3 Summary of rapid condition assessment

Floor #	Max acceleration (mg)	Max displacement (mm)
1	414.79	9.9
2	523.93	13.9
3	385.93	17.8
4	358.97	21.8
5	369.45	25.1
6	493.96	27.4

Table 4 Results comparison between the proposed system and the reference systems (NRMSE)

Floor #	Acceleration	Drift estimation
1	0.0850	0.0858
2	0.0937	0.0848
3	0.0969	0.0606
4	0.1158	0.1160
5	0.1309	0.1103
6	0.1240	0.1709

To demonstrate its functionalities and efficiency, further comparison between the *xShake* and other existing wireless system for seismic SHM is shown in Table 5. Though all of monitoring system employs wireless communication, some systems still rely on wires for power supply, either by direct current (DC) or PoE. These systems do not need power efficiency for earthquake monitoring accordingly, but they may not make the best benefits of cable removal, e.g., ease of installation and associated cost reduction. For the battery-powered monitoring systems including the *xShake*, on-demand sensing techniques are required to achieve power efficiency. Furthermore, real-time data acquisition and visualization are still challenging for some of existing seismic SHM systems; the *xShake* is one of only two systems capable of both live streaming and online condition assessment. In sum, the proposed framework, *xShake*, in this study outperforms existing wireless systems with respect to power efficiency, live streaming, and online condition assessment.

6. Conclusions

In this paper, unique challenges of wireless sensors for seismic monitoring of civil infrastructure have been discussed, including constraints on the power resource and limited network throughput. To address the challenges, an intelligent wireless monitoring system, *xShake*, is developed. In particular, demand-based wireless sensor prototypes are applied as sensor nodes. By incorporating programmable event-based switch, it enables event-triggered sensing with minimal latency, such that earthquakes are not missed. It is in deep sleep mode, consuming ultralow power when no earthquake occurs, addressing the power constraint. Moreover, a live-streaming framework is established to increase the throughput of

Table 5 Comparison of wireless systems for seismic SHM

Characteristics	Low-power WSSN	SOSEWIN	MPwise	EEW-based WSN	Pulse	***xShake***
Study	Torfs *et al.* (2013)	Picozzi *et al.* (2014)	Boxberger *et al.* (2017)	Hung *et al.* (2018)	Wade (2019)	**This study**
Power supply	Battery	DC	DC	Battery	PoE	**Battery**
Sensing scheme	triggered	continuous	continuous	triggered	continuous	**triggered**
Power efficiency	√	×	×	√	×	√
Live streaming	×	√	√	×	√	√
Data visualization	×	×	√	×	√	√

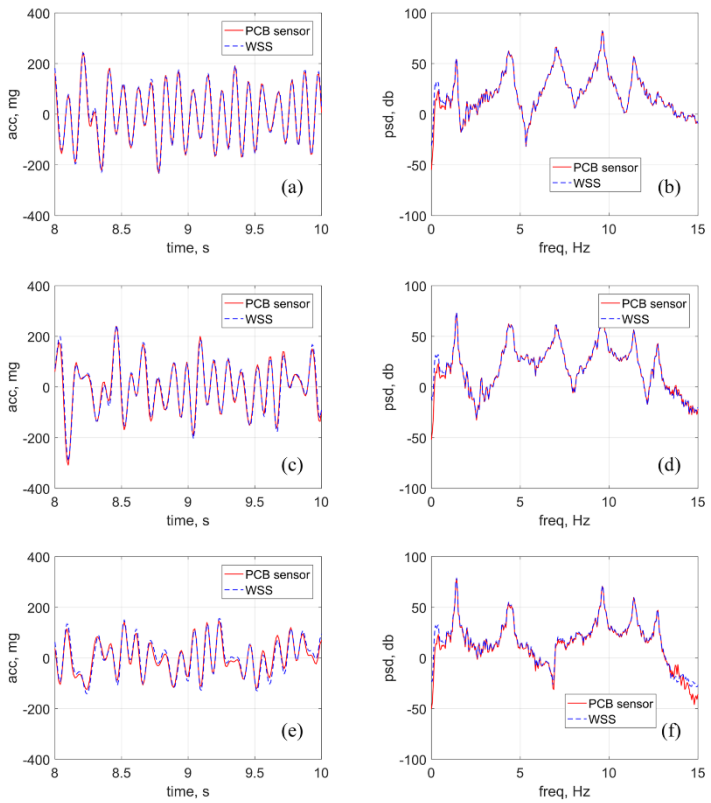

Fig. 14 Acceleration measurements: (a) time history data from Floor #1; (b) PSD from Floor #1; (c) time history data from Floor #3; (d) PSD from Floor #3; (e) time history data from Floor #5; (f) PSD from Floor #5

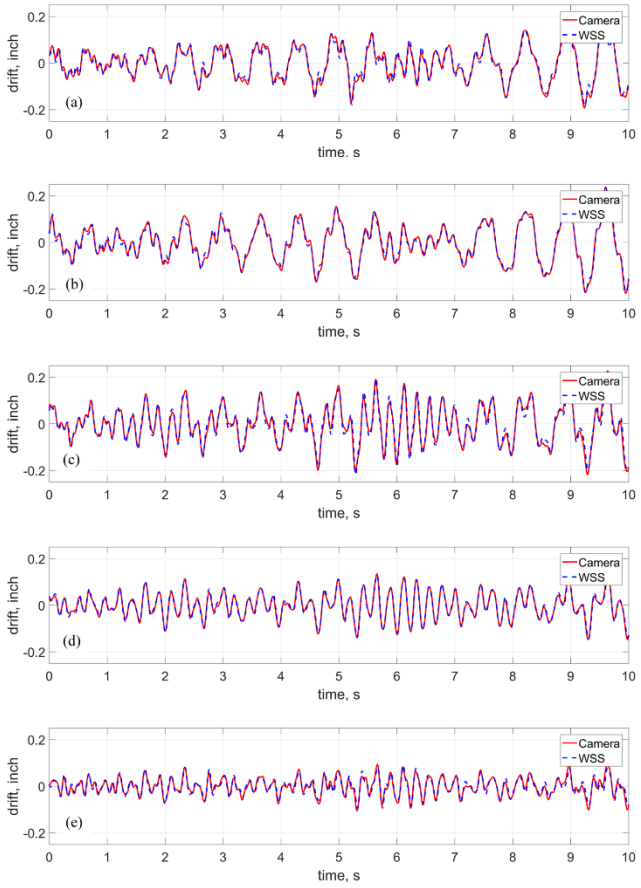

Fig. 15 Interstory drift: (a) Floor 1-2; (b) Floor 2-3; (c) Floor 3-4; (d) Floor 4-5; (e) Floor 5-6

wireless network and eliminate the delay for condition assessment. Specifically, preemptive multitasking is implemented to resolve the task scheduling conflicts within a sensor node, and adaptive staggered TDMA is designed to resolve the radio interference between sensor nodes. As a result, the throughput is significantly increased for real-time data acquisition, which is around 1.5 times of the maximum throughput reported in the literature. In addition, a rapid condition assessment application is developed to realize real-time condition assessment and data visualization. The integrated monitoring system has been validated in a lab test. Test results demonstrate that the *xShake* can detect earthquakes under a minimal power budget, transmit measurement in real-time, and process and visualize the conditions of civil infrastructure in an efficient manner. This intelligent system is versatile and applicable for a broader class of applications, such as bridge impact detection and highway overloads monitoring.

Acknowledgments

The authors gratefully acknowledge the support of this research by NSF SBIR under Grant #1913947, Nazarbayev University Research Fund under Grant #SOE2017003, ZJU-UIUC Institute Research under Grant #ZJU083650, Federal Railroad Administration under Grant #DTFR53-17-C00007, and the China Scholarship Council.

References

Boxberger, T., Fleming, K., Pittore, M., Parolai, S., Pilz, M. and Mikulla, S. (2017), "The multi-parameter wireless sensing system (MPwise): Its description and application to earthquake risk mitigation", *Sensors*, **17**(10), 2400. https://doi.org/10.3390/s17102400

Caicedo, J.M., Clayton, E., Dyke, S.J., Abe, M. and Tokyo, J. (2002), "Structural health monitoring for large structures using ambient vibrations", *Proceedings of the ICANCEER Conference*, Hong Kong, China.

Celebi, M. (2006), "Real-time seismic monitoring of the new Cape Girardeau bridge and preliminary analyses of recorded data: An overview", *Earthq. Spectra*, **22**, 609. https://doi.org/10.1193/1.2219107

Çelebi, M. (2013), *Earthquakes and Health Monitoring of Civil Structures*, Springer, Dordrecht, Netherlands.

Chen, Z and Casciati, F. (2014), "A low-noise, real-time, wireless data acquisition system for structural monitoring applications", *Struct. Control Health Monitor.*, **21**(7), 1118-1136. https://doi.org/10.1002/stc.1636

Cheng, L. and Pakzad, S.N. (2009), "Agility of wireless sensor networks for earthquake monitoring of bridges", *Proceedings of the 6th International Conference on Networked Sensing Systems* (*INSS*), Pittsburgh, PA, USA.

Fu, Y., Mechitov, K.A., Hoskere, V. and Spencer, B.F. Jr. (2016), "Development of RTOS-based wireless SHM system: benefits in applications", *International Conference on Smart Infrastructure and Construction*, Cambridge, UK.

Fu, Y., Hoang, T., Mechitov, K., Kim, J., Zhang, D. and Spencer, B.F. Jr. (2018a), "Sudden-event monitoring of civil infrastructure using demand-based wireless smart sensors", *Sensors*, **18**(12), 4480. https://doi.org/10.3390/s18124480

Fu, Y., Zhu, L., Hoang, T., Mechitov, K. and Spencer, B.F. Jr. (2018b), "Demand-based wireless smart sensors for earthquake monitoring of civil infrastructure", *Proceedings of Sensors and Smart Structures Technologies for Civil, Mechanical, and Aerospace Systems 2018*, Denver, CO, USA.

Fu, Y., Mechitov, K., Hoang, T., Kim, J.R., Lee, D.H. and Spencer, B.F. Jr. (2019), "Development and full-scale validation of high-fidelity data acquisition on a next-generation wireless smart sensor platform", *Adv. Struct. Eng.*, **22**(16), 3512-3533. https://doi.org/10.1177/1369433219866093

Fu, Y., Mechitov, K., Hoang, T., Kim, J.R., Memon, S.A. and Spencer Jr, B.F. (2020), "Efficient and high-precision time synchronization for wireless monitoring of civil infrastructure subjected to sudden events", *Struct. Control Health Monitor.*, **28**(1), e2643. https://doi.org/10.1002/stc.2643

Gomez, F., Park, J.W. and Spencer, B.F. Jr. (2018), "Reference-free structural dynamic displacement estimation method", *Struct. Control Health Monitor.*, **25**(8), e2209. https://doi.org/10.1002/stc.2209

Han, B., Kalis, A., Tragas, P., Nielsen, R.H. and Prasad, R. (2012), "Low cost wireless sensor networks for continuous bridge monitoring", *Proceedings of the 6th International IABMAS Conference on Bridge Maintenance, Safety, Management, Resilience and Sustainability*, Lake Maggiore, Italy.

Hung, S.L., Ding, J.T. and Lu, Y.C. (2018), "Developing an energy-efficient and low-delay wake-up wireless sensor network-based structural health monitoring system using on-site earthquake early warning system and wake-on radio", *J. Civil Struct. Health Monitor.*, **9**(1), 103-115. https://doi.org/10.1007/s13349-018-0315-2

Jang, S., Jo, H., Cho, S., Mechitov, K.A., Rice, J.A., Sim, S.H., Jung, H.J., Yun, C.B., Spencer, B.F. Jr. and Agha, G. (2010), "Structural health monitoring of a cable-stayed bridge using smart sensor technology: Deployment and evaluation", *Smart Struct. Syst., Int. J.*, **6**(5-6), 439-459. https://doi.org/10.12989/sss.2010.6.5_6.439

Kim, S., Pakzad, S., Culler, D., Demmel, J., Fenves, G., Glaser, S. and Turon, M. (2007), "Health monitoring of civil infrastructures using wireless sensor networks", *Proceedings of the 6th International Conference on Information Processing in Sensor Networks*, New York, USA.

Linderman, L.E., Mechitov, K.A. and Spencer, B.F. Jr. (2013), "TinyOS-based real-time wireless data acquisition framework for structural health monitoring and control", *Struct. Control Health Monitor.*, **20**(6), 1007-1020. https://doi.org/10.1002/stc.1514

Liu, Y., Voigt, T., Wirström, N. and Höglund, J. (2018), "ECOVIBE: On-Demand Sensing for Railway Bridge Structural Health Monitoring", *IEEE Internet Things J.*, **6**(1), 1068-1078. https://doi.org/10.1109/JIOT.2018.2867086

Lu, G., De, D., Xu, M., Song, W.Z. and Cao, J. (2010), "TelosW: Enabling ultra-low power wake-on sensor network", *Proceedings of the 2010 IEEE Seventh International Conference on Networked Sensing Systems* (*INSS*), Kassel, Germany.

Lynch, J.P., Wang, Y., Loh, K.J., Yi, J.H. and Yun, C.B. (2006), "Performance monitoring of the Geumdang Bridge using a dense network of high-resolution wireless sensors", *Smart Mater. Struct.*, **15**(6), 1561. https://doi.org/10.1088/0964-1726/15/6/008

McDonnell, P.J., Vives, R. and Linthicum, K. (2017), At Least 3,000 Buildings Found Damaged in Mexico City as Search Narrows for Earthquake's Last Possible Survivors, Los Angeles Times.

Nagayama, T and Spencer, Jr, B.F. (2007), "Structural health monitoring using smart sensors", Newmark Structural Engineering Laboratory, University of Illinois at Urbana-Champaign.

Niu, J., Deng, Z., Zhou, F., Cao, Z., Lui, Z. and Zhu, F. (2009), "A

structural health monitoring system using wireless sensor network", *Proceedings of the 5th International Conference on Wireless Communications*, *Networking and Mobile Computing 2009*, Beijing, China.

Okada, K., Nakamura, Y. and Saruta, M. (2009), "Application of earthquake early warning system to seismic-isolated buildings", *J. Disaster Res*., **4**(4), 242-250. http://doi.org/10.20965/jdr.2009.p0242

Picozzi, M., Milkereit, C., Fleming, K., Fischer, J., Jaeckel, K.H., Bindi, D., Parolai, S. and Zschau, J. (2014), *Early Warning for Geological Disasters*, Springer, Berlin, Heidelberg, Germany.

Popovic, N., Feltrin, G., Jalsan, K.E. and Wojtera, M. (2017), "Event-driven strain cycle monitoring of railway bridges using a wireless sensor network with sentinel nodes", *Struct*. *Control Health Monit*., **24**, e1934. http://doi.org/10.1002/stc.1934

Potenza, F., Federici, F., Lepidi, M., Gattulli, V., Graziosi, F. and Colarieti, A. (2015), "Long-term structural monitoring of the damaged Basilica S. Maria di Collemaggio through a low-cost wireless sensor network", *J. Civil Struct*. *Health Monitor*., **5**, 655-676. http://doi.org/10.1007/s13349-015-0146-3

Spencer, B.F., Park, J.W., Mechitov, K.A., Jo, H. and Agha, G. (2016), "Next generation wireless smart sensors toward sustainable civil infrastructure", *Proceedings of Sustainable Civil Engineering Structures and Construction Materials*, Bali, Indonesia.

Sutton, F., Da Forno, R., Gschwend, D., Gsell, T., Lim, R., Beutel, J. and Thiele, L. (2017), "The Design of a Responsive and Energy-efficient Event-triggered Wireless Sensing System", EWSN, Uppsala, Sweden.

Torfs, T., Sterken, T., Brebels, S., Santana, J., Hoven, R., Spiering, V., Bertsch, N., Trapani, D. and Zonta, D. (2013), "Low power wireless sensor network for building monitoring", *IEEE Sensors J*., **13**(3), 909-915. http://doi.org/10.1109/JSEN.2012.2218680

Wade, L. (2019), Is Your Building Safe After an Earthquake? These Cheap Sensors Could Tell You. Science.

Wang, Y., Lynch, J.P. and Law, K.H. (2007), "A wireless structural health monitoring system with multithreaded sensing devices: design and validation", *Struct*. *Infrastruct*. *Eng*., **3**(2), 103-120. https://doi.org/10.1080/15732470600590820

Whelan, M.J. and Janoyan, K.D. (2009), "Design of a robust, high-rate wireless sensor network for static and dynamic structural monitoring", *J. Intell*. *Mater*. *Syst*. *Struct*., **20**(7), 849-863. https://doi.org/10.1177/1045389X08098768

Xiao, H., Lu, C. and Ogai, H. (2012), "A multi-hop low cost time synchronization algorithm for wireless sensor network in bridge health diagnosis system", *Proceedings of IEEE International Conference on Embedded and Real-Time Computing Systems and Applications*, Washington, DC, USA.

Xiao, H., Lu, C. and Ogai, H. (2017), "A new low-power wireless sensor network for real-time bridge health diagnosis system", *Proceedings of 56th Annual Conference of the Society of Instrument and Control Engineers of Japan* (*SICE*), Kanazawa, Japan.

Yamazaki, F. (2001), "Seismic monitoring and early damage assessment systems in Japan", *Progress Struct*. *Eng*. *Mater*., **3**(1), 66-75. https://doi.org/10.1002/pse.75

Yamazaki, F., Katayama, T. and Yoshikawa, Y. (1994), "On-line damage assessment of city gas networks based on dense earthquake monitoring", *Proceedings of 5th U.S. National Conference on Earthquake Engineering*, Chicago, IL, USA.